



OPEN ACCESS

EDITED BY

Ge Yang,
North Carolina State University,
United States

REVIEWED BY

Jafar Iqbal Khan,
Northwestern University, United States
Zhaolai Chen,
Shandong University, China

*CORRESPONDENCE

Dan Xie,
✉ xiedan@tsinghua.edu.cn
He Tian,
✉ tianhe88@tsinghua.edu.cn
Yi Yang,
✉ yiyang@tsinghua.edu.cn
Tian-Ling Ren,
✉ RenTL@tsinghua.edu.cn

[†]These authors have contributed equally to this work

SPECIALTY SECTION

This article was submitted to
Radiation Detectors and Imaging,
a section of the journal
Frontiers in Physics

RECEIVED 02 December 2022

ACCEPTED 23 March 2023

PUBLISHED 05 April 2023

CITATION

He Y, Wang Z, Wang Z, Dun G-H, Geng X,
Wang C, Du J, Guo T, Xie D, Tian H, Yang Y
and Ren T-L (2023), Perovskite band
engineering for high-performance X-
ray detection.
Front. Phys. 11:1114242.
doi: 10.3389/fphy.2023.1114242

COPYRIGHT

© 2023 He, Wang, Wang, Dun, Geng,
Wang, Du, Guo, Xie, Tian, Yang and Ren.
This is an open-access article distributed
under the terms of the [Creative
Commons Attribution License \(CC BY\)](https://creativecommons.org/licenses/by/4.0/).
The use, distribution or reproduction in
other forums is permitted, provided the
original author(s) and the copyright
owner(s) are credited and that the original
publication in this journal is cited, in
accordance with accepted academic
practice. No use, distribution or
reproduction is permitted which does not
comply with these terms.

Perovskite band engineering for high-performance X-ray detection

Yichu He^{1,2†}, Zeshu Wang^{1,2†}, Zi Wang^{1,2†}, Guan-Hua Dun^{1,2},
Xiangshun Geng^{1,2}, Chunlin Wang^{1,2}, Jingbo Du^{1,2}, Tianyu Guo^{1,2},
Dan Xie^{1,2*}, He Tian^{1,2*}, Yi Yang^{1,2*} and Tian-Ling Ren^{1,2*}

¹School of Integrated Circuits, Tsinghua University, Beijing, China, ²Beijing National Research Center for Information Science and Technology (BNRist), Tsinghua University, Beijing, China

Perovskite-based X-ray detector, which is widely applied in fields of scientific research and medical diagnosis, has drawn much attention for its superior optoelectrical properties. To improve the detection performance, band engineering is becoming the hot topic for perovskite properties modulation. In this article, we review the recent progress of perovskite-based X-ray detectors with band engineering process from three aspects, which are background introduction, band theory of heterojunction devices, and optimized electrode contact devices. Lastly, research status and strategies are summarized and perspectives of future progress are analyzed. We hope this review can provide constructive instructions and suggestions for future development of band engineering for perovskite-based high-performance X-ray detector.

KEYWORDS

perovskite, band engineering, x-ray detector, heterojunction, electrode contact

1 Introduction

X-ray detection, which transfers X-ray irradiance to measurable current signals, is attracting much attention for its wide application from space exploration, scientific research, flaw detection to people's daily life, say medical X-ray imaging. The X-ray source, however, may impact on human health and damage the equipment due to radiation leakage. Hence, X-ray detector with high sensitivity and response speed is expected [1]. In terms of pattern in which X-ray are converted into electrical signals, direct conversion detection exhibits higher efficiency than indirect one. Because of direct conversion effect, X-ray signals can be transferred to current signals directly for reinforced transportation of electrons and holes under external bias [2], for which signal-noise ratio (SNR) and response time can be reduced. X-ray detection materials are proven to show such qualities as: (1) heavy atoms for efficient X-ray absorption; (2) high resistivity and low dark current to make device with low leakage [3]; (3) relatively high $\mu\tau$ product to facilitate the transportation and collection of carriers. μ and τ represent carrier mobility and carrier lifetime respectively [4]; (4) considerable stability [5]. The device should be persistent enough to maintain a low surface leakage current.

Recently, metal halide perovskite (MHP) has drawn much attention to X/gamma-ray detection ascribing to its attractive composition and superior physical properties. Intrinsically, the composition and structure based on MHP are reconfigurable for low power [6, 7]. And great tolerance of material itself is exhibited for high impurity states to realized a long-term working time. In terms of fabrication, MHP is compatible with Si

fabrication for pixelation integration and can be conducted at room temperature at a bargain price. Besides, high resolution and sensitivity of MHP open a avenue for X-ray detector of high performance. Nowadays, the maximum sensitivity of perovskite X-ray detectors exceeds that of commercial α -Se-based X-ray detectors by 6-7 orders of magnitude, which is significantly lower than the dose-rate standard required for medical imaging [8, 9].

Though perovskite X-ray detector has fulfilled current requirements from the perspective of sensitivity and detection, stability remains a major obstacle to its commercial application. One of the most difficult challenges affecting the stability of perovskite is ion migration in the very material. Notably, ion migration is directly related to the surface defects [10]. In perovskite crystals, ion migrates through Schottky defects, Frankel defects and other defects. Especially for polycrystalline films, the grain boundary and crystal surface are relatively open. In addition to point defects, the activation energy is lower than that in the crystal. Accordingly, the grain boundaries are significant channels for ion migration. Undesirable defects and surface trap states will considerably aggravate current drift and dark current.

Hence, by constructing the same dimension perovskite heterojunction, suboptimal carrier transport characteristics caused by defects can be improved. For instance, a lateral grown pn heterojunction of p-type $\text{CH}_3\text{NH}_3\text{PbBr}_3$ (MAPbBr₃)/n-type $\text{CH}_3\text{NH}_3\text{PbCl}_3$ (MAPbCl₃) can effectively passivate surface defects of pristine materials due to excellent and robust lattice matching [11]. Besides, the designed heterojunction endows the existence of built-in electric field and further reduces dark current to perform a favorable carrier transport characteristic, which guarantees for excellent photoelectric performance.

As for perovskite single crystals (SC), the ion migration barrier is generally increased by passivation of halogen vacancy [12]. For example, the ion migration of $\text{Cs}_2\text{AgBiBr}_6$ is inhibited by heteroepitaxy BiOBr growth so that the signal drift of X-ray detector prepared by BiOBr is three orders of magnitude lower than that of previous detectors [13]. For polycrystalline thick film (over 1 μm) [14], similar effect can be realized by increasing the density of polycrystalline film to reduce the cavity, passivate grain boundaries and introduce the quasi two-dimensional structure of dark current [15], adding suitable polymer barrier layer and so on. Additionally, organic amine ion inhibition can also be introduced [16], which increases the ion migration barrier by increasing the chain length.

High sensitivity and low dose rate of 3D perovskite X-ray detectors promise an expected platform to study intrinsic characteristic of material and attracts increasingly attention [17]. Disappointingly, three-dimensional perovskite has the limitation of tolerance factor, leading to the obstacle of instability [18]. The presence of three-dimensional perovskites limit the serve life of the products and hampers the desire to significantly reduce the X-ray dose in medical imaging. Surprisingly, 2D perovskite counterparts separated from long-chain organic cations reveal advanced features in suppressing ion migration, which is at large applied bias. Therefore, in recent years, the establishment of heterogeneous structures with different dimensions is also one of the most effective and widely used means to settle the instability problem of perovskites [7]. At present, abundant new heterojunction perovskite materials with

diverse composition and structural dimensions, such as 2D $(\text{FPEA})_2\text{PbBr}_4$ /3D FAPbBr_3 fabricated through epitaxy growth method, have been reported [19].

Integrating three-dimensional with two-dimensional perovskite materials make it possible to realize a X-ray detector material with high carrier mobility [20], large exciton binding energy and large $\mu\tau$ product [3, 4]. And reliable stability [5], effective charge transfer and tunable band gap [6] with different number of layers guarantee that the mixed perovskite X-ray detector has great potential in preferred properties.

In the context, this work aims to review previous explorations on the optimization of perovskite-based X-ray detectors through energy band engineering, which is an efficient carrier management strategy. To overcome MHPs' intrinsic limitations such as impurity defects, ions migration, it is a profound way to improve the combination of different heterojunctions. This paper involves two parts: the band engineering with heterojunction and the energy band optimization of the contact with metal electrodes. By retrospectively the energy band characteristics after the integration of different materials and summarizing their alterable characteristics, it is expected to provide guidance for the fabrication of X-ray detectors in the future, as well as the design and preparation of other materials such as LED, solar cells etc., so as to achieve photoelectric conversion with higher performance and accelerate the application and development of perovskites in years to come.

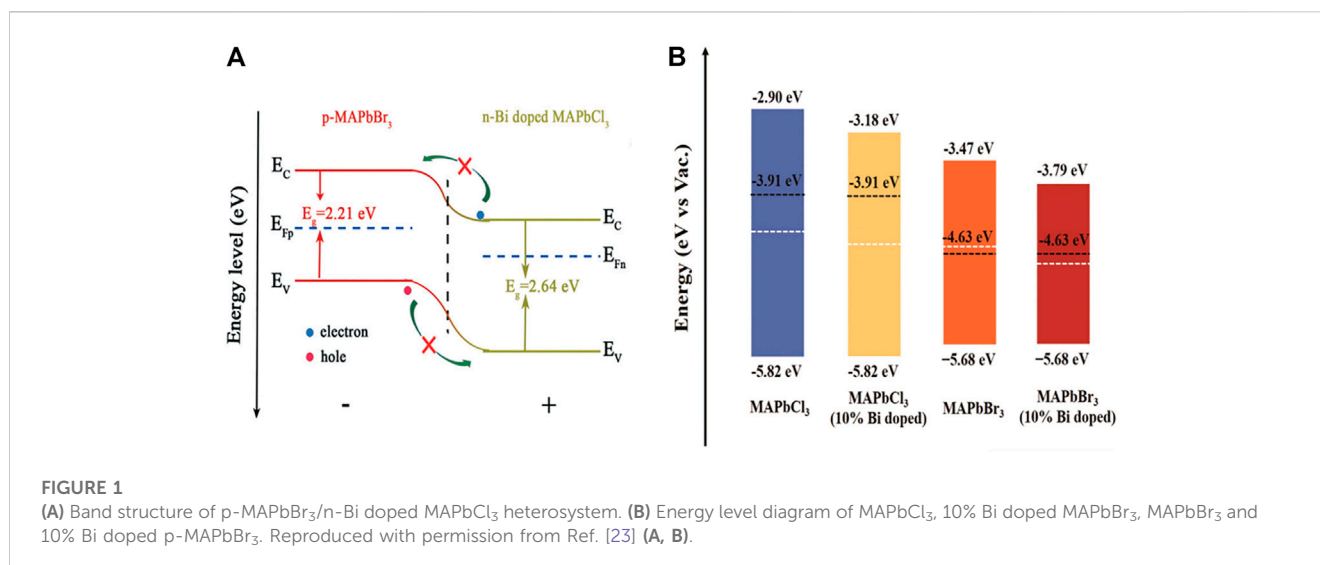
2 Band engineering theory

The band engineering of semiconductors can be categorized into two aspects [21, 22]:

one refers to bandgap pattern engineering. By means of doping, energy band structure can be modified to modulate the transportation of carriers a great extent, resulting in high detection performance. Another is bandgap structure engineering. Semiconductors with different bandgap can be tailored to influence the transportation of charge carriers between materials, for which the optoelectronic (electric and optical) properties can be optimized.

2.1 Bandgap pattern engineering with doping process

Rational doping methodology is meaningfully demanded to optimize the performance of materials. With the development of semiconductor engineering and the profound study of doping for band structure tailoring, it is found that dopant provides perovskite intrinsic layer with electrons while the ionized impurities work as scattering center to promote electron migration. Since the electron and scattering centers are separated, the dilemma of both improving the carriers concentration and materials mobility can be solved. Doping can fairly improve the X-ray detection performance of perovskite, although partially occupied impurity states will be introduced and work as recombination center for X-ray-generated electron/hole pairs to reduce their separation and hence the photocurrent. Excessive concentration and overthick layer of doping may lead to increased leakage current and resistivity, respectively. Consequently, appropriate approach of



doping is desired for electron/hole pairs recombination center can be eliminated partially, leading to higher photocurrent.

Yan *et al.* [11] fabricated a p-MAPbBr₃/n-MAPbCl₃ heterojunction photodetector with a sensitivity of 26.8 mA W⁻¹ and a response time of 8 μs. However, organic semiconductor shows low response speed due to its low carriers mobility and high exciton binding energy. Inspired by doping Bi³⁺ in MAPbBr₃ and CsPbBr₃, Pan and coworkers [23] improved response speed, n-type conductivity and within-gap trap states of MAPbCl₃ SC through Bi³⁺ interstitial doping [24, 25]. Epitaxial growth was utilized to fabricate Bi³⁺-doped MAPbCl₃/MAPbBr₃ pN heterojunction (Figure 1A). As can be seen in Figure 1B, Bi³⁺ doping narrows the band gap. The transmission of electrons and holes was prohibited at reversed bias due to enhancement of carrier diffusion by Bi³⁺ doping. The dark current can be effectively reduced, leading to long term current stability and low noise. By modulating doping structure, electrons in MAPbCl₃ were transferred to MAPbBr₃, from which the number of carriers was increased without the drop of mobility. This benefited the promotion of response speed. X-ray detector fabricated by p-MAPbBr₃/Bi³⁺-doped MAPbCl₃ has a remarkable advantage of high sensitivity ($0.72 \times 10^3 \mu\text{C Gyair}^{-1} \text{cm}^{-2}$) and short response time (4.89 μs) compared with undoped one.

Thus, as a promising methodology, doping reasonably can ensure the increase of carriers concentration and materials' mobility, contributing to the reduction of dark current and the enhancement of sensitivity. In terms of future work, it has been suggested that two or more metal dopants, such as Cu, Mn, In, Ga and so on, could be applied simultaneously to compensate the partially doping impurity states [26] and tail the band.

2.2 Bandgap structure engineering with heterojunction

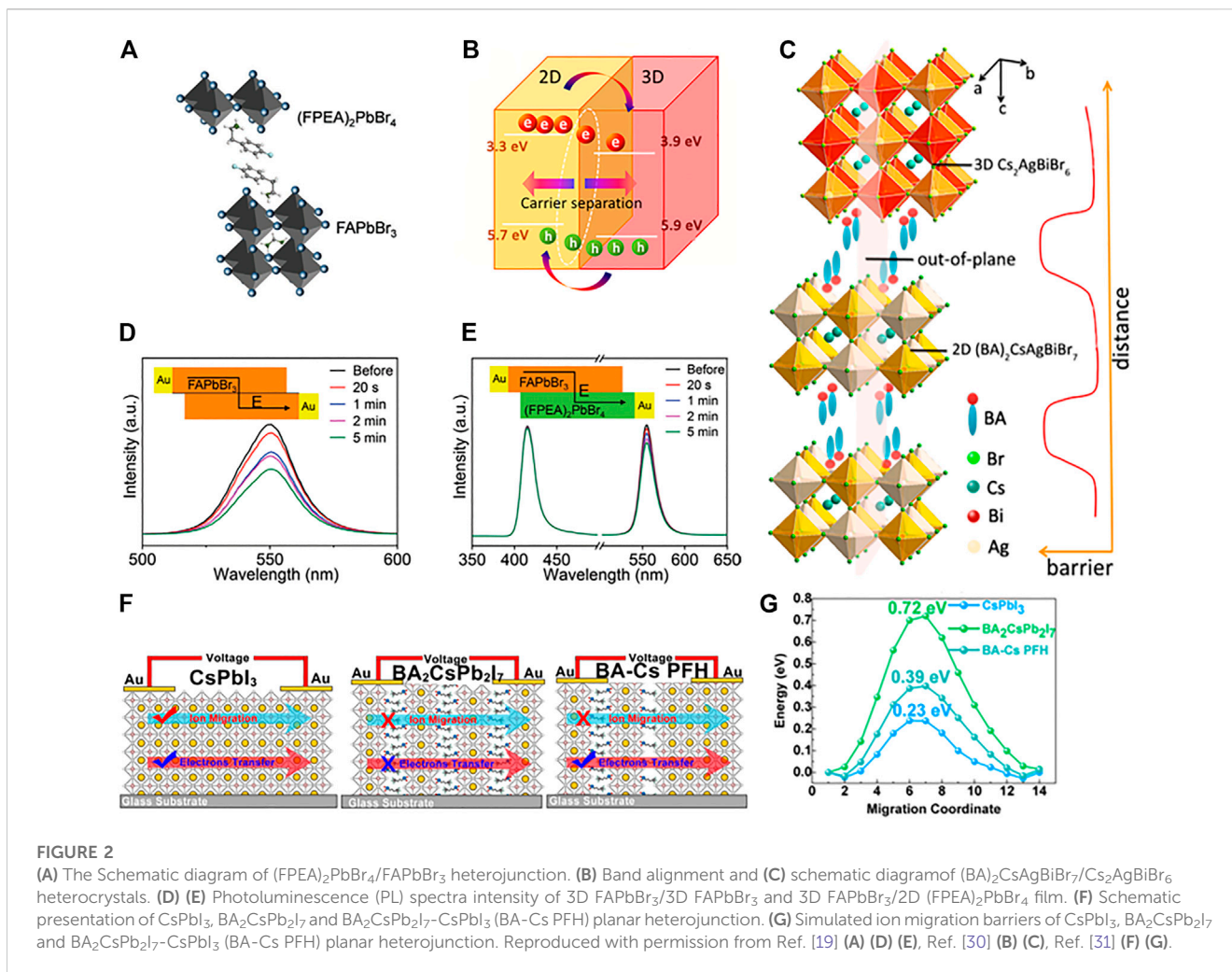
Recently, intrinsic monophasic semiconductors without doping have been widely investigated. But intrinsic limitations of single

material restrict the development of X-ray detection. To combine materials with various properties, heterojunction has attracted much attention to be fabricated for detection performance enhancement [27, 28].

2.2.1 2D/3D perovskite heterojunction

3D perovskite continues to dominate the X-ray detector research attributed to its superior X-ray sensitivity. Unfortunately, the ion migration in 3D perovskite is especially distinct, particularly occurring on free surfaces and grain boundaries. The bonding of surface atoms is weak due to the breaking of chemical bonds [29]. In contrast, 2D perovskite with high resistance ensures the suppression of ion migration effectively and enlarges the energy barrier of hole injection without affecting carrier extraction. It would be a novel idea to grow 2D perovskite epitaxially on 3D perovskite to mitigate ion migration. However, the voids between 2D/3D perovskite heterojunction are the obstacles for long-term stability. Accordingly, organic spacer can be applied in filling voids of heterojunction to form compact interface, contributing to the increase of performance.

3D FAPbBr₃ SC (single crystal) serves as a distinguished material for X-ray detection due to its high $\mu\tau$ product. But ion migration is the main downside at external bias, leading to severe dark current drift and device noise. Therefore, He *et al.* [19] utilized long-chain organic cation FPEA⁺ to separate octahedral sheet [PbBr₆]⁴⁻, forming 2D epitaxial layer (FPEA)₂PbBr₄ on 3D FAPbBr₃ SC surface tightly shown in Figure 2A. In contrast, 2D (FPEA)₂PbBr₄ SC can deactivate surface defects of 3D FAPbBr₃ using wide gap detect deactivation effect. Through space-charge limited current (SCLC) technique, it was observed that the detect density ($3.18 \times 10^9 \text{cm}^{-3}$) of heterojunction was decreased dramatically compared with FAPbBr₃ ($4.70 \times 10^9 \text{cm}^{-3}$). With the contrast of investigation of 3D/3D and 3D/2D's photoluminescence (PL) spectra intensity after 5 min polarization, it was demonstrated that PL in 3D/3D film quenched severely while in 3D/2D film, however, few quench of PL intensity of 2D perovskite was obtained (Figures 2D,E). PL intensity of 3D perovskite also retains 80% of original value,



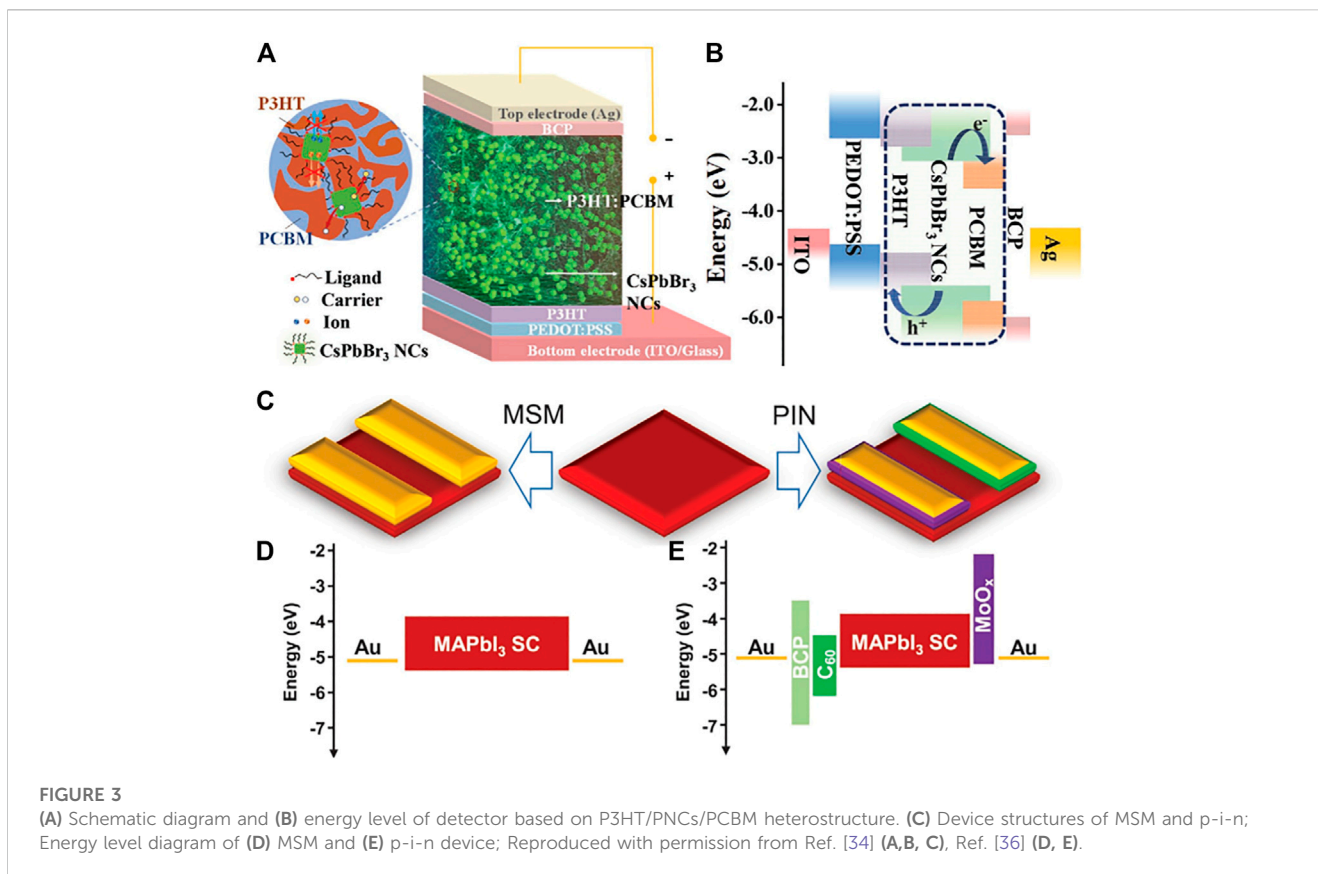
proving that the ion migration was inhibited effectively. Meanwhile, the long-term job security was guaranteed. This technique enabled the biased heterojunction had advanced performance in X-ray detecting application.

To modify the voids of 2D/3D heterojunction, Zhang *et al.* [30] regarded (BA)₂CsAgBiBr₇ as seed crystal, guiding its *in situ* epitaxial growth on 3D Cs₂AgBiBr₆ to form vertical type-II heterojunction (Figure 2B). With the decrease of temperature, nucleus expanded horizontally. Vertical inorganic [Ag(Bi)Br₆]_∞ layer was inhibited by large-volume BA⁺, separating the inorganic layers as shown in Figure 2C. New (BA)₂CsAgBiBr₇ crystals can fill voids inside heterojunction, forming sharp interface with intensive adhesion at atomic scale. 2D organic spacer was integrated with (BA)₂CsAgBiBr₇ to induce steric hindrance, increasing the activation energy to resist uncontrollable ion migration. Meanwhile, the formation of pn junction with Cs₂AgBiBr₆ as p-type and (BA)₂CsAgBiBr₇ as n-type yields the existence of built-in potential. Thus, X-ray generated carriers can be separated and transported effectively, and device noise can be also reduced, from which the heterojunction crystal can be driven by itself. The device can detect X-ray directly without external power supply, reducing dark current and dark current drift dramatically. The X-ray

detector showed a low dark current of 3.2×10^{-2} pA and a sensitivity of $206 \mu\text{C Gyair}^{-1} \text{cm}^{-2}$.

In other cases, Xu *et al.* [31] proposed the trade-off between BA₂CsPb₂I₇ and 3D homologs CsPbI₃. The authors designed asymmetrical plane film structure of BA₂CsPb₂I₇-CsPbI₃ perovskite film heterojunction (BA-Cs PFH) as shown in Figure 2F. For typical BA₂CsPb₂I₇, ion migration can be suppressed to reduce dark current effectively due to quantum confinement effect and dielectric confinement of organic molecular layer (Figure 2G). Thus, the detector showed a high on-off ratio of ~308 and detectivity of $0.092 \mu\text{Gyairs}^{-1}$. Meanwhile, BA₂CsPb₂I₇ minimized the leakage current. Considering the intrinsic defects and the capture and relief of ion migration in crystal lattice, it was demonstrated that BA-Cs PFH exhibited higher sensitivity than CsPbI₃'s ($<0.1\text{s}$ vs. $\sim 3\text{s}$).

Herein, the inhibited ion migration is prone to appear in 2D/3D structure which acts as the foundation for X-ray detector with high performance. And with the addition of organic molecular layer, halogen ion migration of inorganic halogen perovskite is suppressed. Notably, as the thickness of the organic molecular layer increases, the number of transferred electrons may decrease, so only a moderate value can be taken.

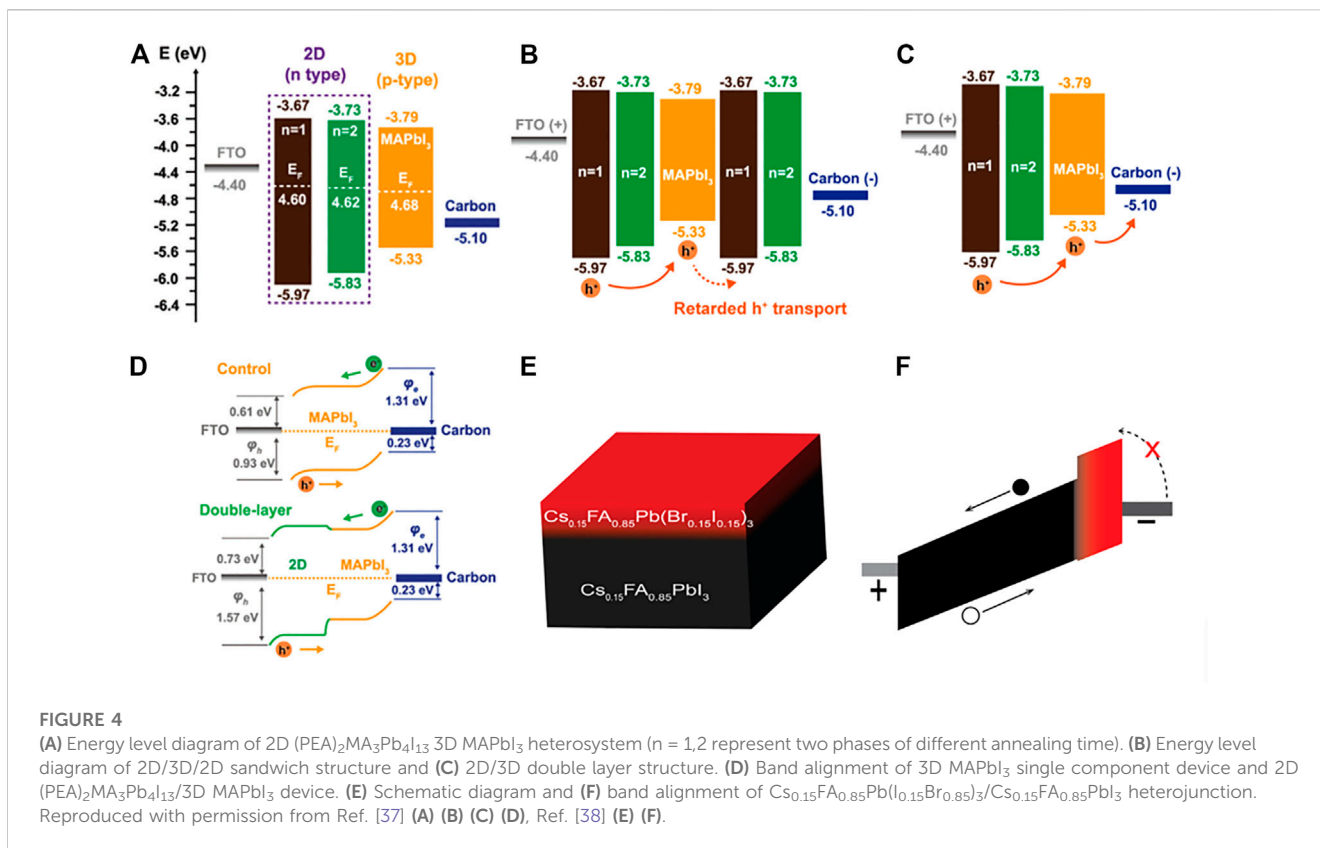


2.2.2 Device structure design

Detectors with novel structure, such as double layers heterostructure, p-i-n structure and so on, exhibit great potential for higher X-ray detection capability. Double heterostructure plays a dominant role in blocking carriers that generated inside the device structure [32], and only carriers that photogenerated within the top absorption layers can be completely depleted and collected, leading to a fast response [33]. With appropriate band direction design, double heterostructure can be obtained. Not only X-ray generated carriers transportation can be enhanced but also ion migration can be suppressed. Wei *et al.* [34] fabricated X-ray detector based on poly (3-hexylthiophene-2,5-diyl) (P3HT)/CsPbBr₃ perovskite nanocrystals (PNCs)/(6,6)-Phenyl-C₆₁ butyric acid methyl ester (PCBM) as two type-II heterostructures [Figure 3A]. Since the X-ray was sensitized, carriers generated by X-ray in PNCs can be separated and transported to P3HT and PCBM quickly due to the alignment of band structure [Figure 3B]. It was demonstrated that the sensitivity of P3HT:PCBM/CsPbBr₃ hybrid device was increased by an order compared with P3HT:PCBM and CsPbBr₃ devices. Sensitivity of double heterostructure exceeded two orders of magnitudes than PNC nano hybrid film due to self absorption effect, exhibiting its efficient detecting capability. Surrounding organic matrix can block the ion migration because it hindered the route of ion migration in organic net physically, ensuring higher electric field to enhance the efficiency of charge collection. This benefited the improvement of X-ray response and

realization of low dark current drift ($3.57 \times 10^{-9} \text{ cm s}^{-1} \text{ V}^{-1}$). Thus, the device showed a high X-ray generated current and low dark current, 30 times lower than PNC film $1.06 \times 10^{-7} \text{ cm s}^{-1} \text{ V}^{-1}$.

It is shown in Figure 3C that p-i-n or metal-semiconductor-metal (MSM) structure photodetectors with high-speed and low-noise operation are widely employed in X-ray detector to enhance the sensitivity [35]. Accordingly, p-type and n-type charge transformation layers can be introduced to fabricate novel X-ray detector with p-i-n structure to reduce interface reaction and promote effective separation of carriers. This served a practical methodology to design devices with high responsivity and SNR. Song *et al.* [36] proposed X-ray detector based MAPbI₃ SC. The charge transformation layer was inserted between MAPbI₃ and Au to fabricate a MSM structure (Figure 3D). On the other hand, BCP/C₆₀ and MoO_x were applied in p-type and n-type carriers transportation layers, which were combined with MAPbI₃ SC to form p-i-n structure as shown in Figure 3E. By comparing these two structures, it was found that the ion migration energy of p-i-n structure is higher than that of MSM structure (405 meV vs. 268 meV). P-i-n structure displays excellent ion migration inhibition effect at reversed bias. At the same time, separating perovskite from electrode contact can reduce the polarity induced by electrochemistry contributing to charge inhibition. As a result, the dark current of p-i-n device ($\sim 1 \text{ nA}$) was lower three orders of magnitude compared with original condition. It made it possible to fabricate X-ray detector with high sensitivity ($5.2 \times 10^6 \mu\text{C Gyair}^{-1} \text{ cm}^{-2}$) and low detectivity ($0.1 \text{ nGyair s}^{-1}$).



For the above MSM structure, the time of carriers collection was excessively long under the reach-through bias. Even with a higher bias, the collection time still maintains long owing to the delay of carriers deep in semiconductor layer. More severely, thermionic emission and Schottky contact tunneling are two main factors to increase the dark current. Hence, p-i-n has obvious superiority of quick response over MSM. Generally, introducing novel structure to X-ray detector is a promising way to optimize the performance of the detector, which can reduce the ion immigration and enhance the carriers transportation to increase the SNR.

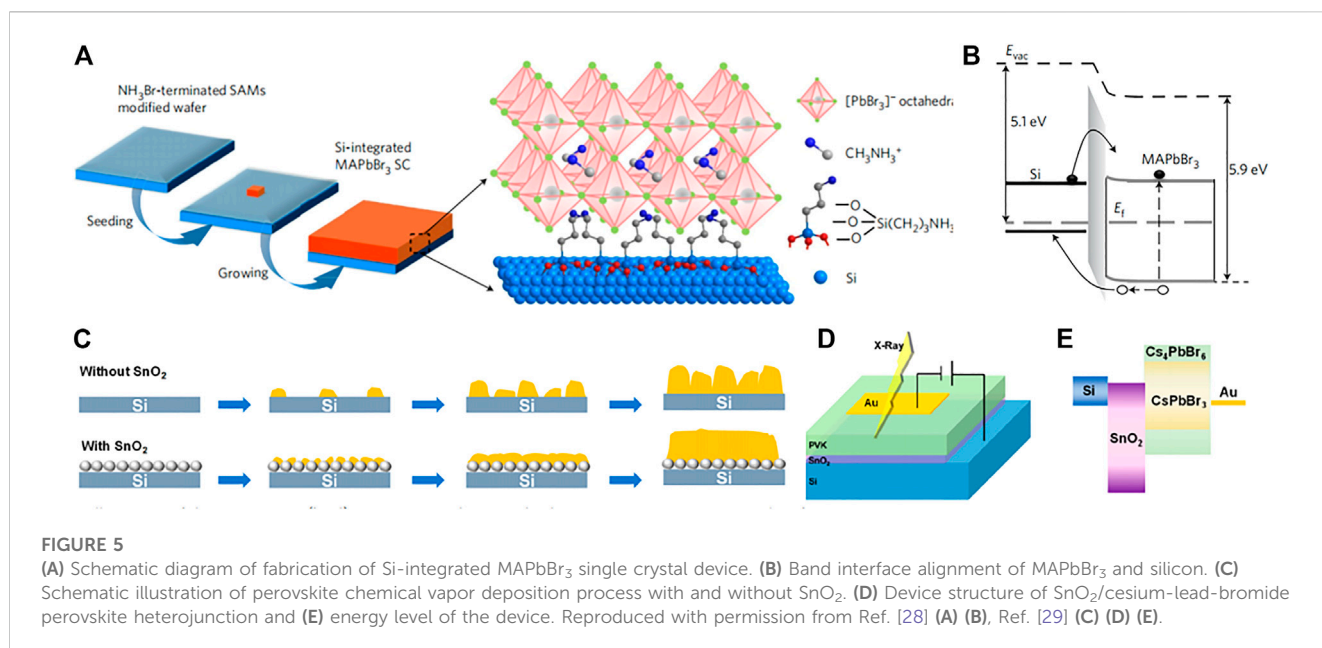
2.2.3 Components modification

The gradient band distribution of low dimensional perovskite benefits the alignment of heterojunction band edges, facilitating the carriers transportation. As shown in Figure 4A, Xu *et al.* [37] proposed new formula through construction of two phases 2D (PEA)₂MA₃Pb₄I₁₃ (PEA = 2-phenylethylammonium, MA = methylammonium) and 3D MAPbI₃ cascade. The contact of low dimensional (PEA)₂MA₃Pb₄I₁₃ and positive electrode fluorine-doped SnO₂ (FTO) glass made VBM boundary deeper as shown in Figure 4D. Accordingly, amplified voids implantation energy decreased dark current, benefiting the enhancement of SNR. Although the slow response of X-ray can be mitigated by applying high electric field, the sensitivity of double layers perovskite detector based on effective holes circulation exhibited two orders of magnitude higher compared with 2D/3D and 2D/3D/2D sandwich structure as shown in Figures 4B,C.

In addition to construct cascade structure, introducing wide gap layer at the interface between perovskite and electrode can generate higher potential barrier, prohibiting the injection of holes or electrons to suppress dark current. Zhou *et al.* [38, 39] also reported

Cs_{0.15}FA_{0.85}Pb(I_{0.15}Br_{0.85})₃/Cs_{0.15}FA_{0.85}PbI₃ heterojunction adopting dip coating process (Figure 3E). The device can inhibit dark current under X-ray illumination at reversed bias. As shown in Figure 3F, perovskite with wide band gap Cs_{0.15}FA_{0.85}Pb(I_{0.15}Br_{0.85})₃ showed higher electrons injection barrier (~1.0eV). Utilizing solar cell capacitance simulator, it turned out that calculated dark current density of heterojunction within WGB can be reduced to 0.73 ± 0.05 nA cm⁻² due to the obstacle of electrons, which was two orders of magnitude lower than any single material at reversed bias.

Additionally, except the research about heterojunction based on perovskite such as p-MAPbBr₃/n-CsPbBr₃ [39], non-perovskite semiconductors can also provide abundant band structure candidates, including CuI [39], Te [40], etc. Although the above researches have been achieved, there still exist massive opportunities for future explore. The type-II heterojunction can be deemed as a reliable guideline of band structure design. On account of band alignment [41], the heterojunction promotes the separation of X-ray generated electrons/holes to realize higher detection performance. In terms of materials selection, it is worthwhile to exploit wide band gap materials to block carriers injection from the interface between the electrode and perovskite, even resulting in increase of trap density. And the other potential materials in this fields are ranging from organic material, inorganic salts, 2D materials and other related materials [42].



2.2.4 Interface modification

Organic molecules have been developed as electrons donor or acceptor, which can serve as middle layer for construction of dipoles to increase adhesion. Meanwhile, this dipole can modulate energy barriers and band alignment. As shown in Figure 5A, Wei *et al.* [28] applied brominated (3-aminopropyl) triethoxysilane molecule (APTES) as middle layer in MAPbBr₃ integrated on Si device. Ammonium bromide group built up mechanical and electrical connection with MAPbBr₃ crystals inherently. The shift of brominated APTES dipole's vacuum level promoted the band alignment of Si and MAPbBr₃, making a possibility of less rectification contact as shown in Figure 5B. This inserted APTES dipole layer exhibited high energy barrier for electrons injection and low energy barrier for holes extraction, leading to low dark current. The reduced dark current ensured the proper work of device at higher bias. Thus, the device exhibited a high sensitivity of $2.1 \times 10^4 \mu\text{C Gyair}^{-1} \text{cm}^{-2}$ under 8 keV X-ray radiation.

Tons of sub-micro defects were distributed on both sides of perovskite, giving rise to interface voltage loss and the reduction of perovskite's stability. To deactivate defects and promote charge transportation, inserting electron (SnO₂, TiO₂, ZnO) and hole (NiO_x) transportation layer become necessary [43]. As shown in Figure 5C, Li *et al.* [30] inserted SnO₂ nano layer between CsPbBr₃ perovskite to form heterojunction. With the introduction of SnO₂ nucleus, surface energy of system was reduced. In the meanwhile, perovskite prior deposition speed was significantly boosted, obtaining lower density defects and thicker film to suppress ion migration. Besides, due to the existence of electrons transportation layer, electron collection from perovskite layer to negative electrode can be enhanced, [Figure 5D, E] deriving X-ray detector with a high sensitivity of $2,930 \mu\text{C Gyair}^{-1} \text{cm}^{-2}$ and low detectivity of $120 \text{ nGyair s}^{-1}$.

In other ways, polishing method like O₃-UV treatment can be applied to passivate surface defects. Feng *et al.* [44] fabricated X-ray

photodetector based on PEDOT:PSS/MAPbBr₃/C₆₀/BCP as shown in Figures 6A,B. PEDOT:PSS and C₆₀/BCP serve as electron and hole transportation layers respectively to enhance charge generation. In this research, O₃-UV treatment were applied on MAPbBr₃ SC's surface to passivate traps, leading to a drop of trap density from $2.59 \times 10^{10} \text{cm}^{-3}$ to $1.69 \times 10^{10} \text{cm}^{-3}$. Consequently, the detector with high photocurrent and low dark current was realized, as shown in Figure c d, which is consistent with low defect density.

Essentially, both the insertion of SnO₂ and the addition of small organic molecules are a means of defects passivation. They are regarded as modifiers of electrical properties, such as carrier mobility and work function. Foremost, more inorganic salts, small organic molecules and even other polymers deserves to be exploited for interface modification. And the approaches such as O₃-UV treatment are value to utilize for passivating surface defects

3 Perovskite X-ray detectors with Electrode contact

Electrodes play an important role in improving performance of X-ray detectors. When selecting suitable electrodes, chemical stability and metal-semiconductor contact must be taken into consideration. For example, Al and Ag are more likely to react with halide perovskites compared to Au [36]. Besides, electrode contact technologies mainly used in perovskite X-ray detectors are Ohmic contacts and Schottky contacts. Ohmic contacts promote charge carrier transport. Detectors with Ohmic contacts usually work at low bias voltage, which means charge carriers are easily lost due to capture and recombination, and causes incomplete charge collection, resulting in poor energy resolution. To enhance charge collection, large bias is needed. However, it will cause the increased dark current. Compared to Ohmic detectors, Schottky detectors have higher Schottky barriers that create a built-in electric field, allowing them working as self-powered devices. Moreover, larger

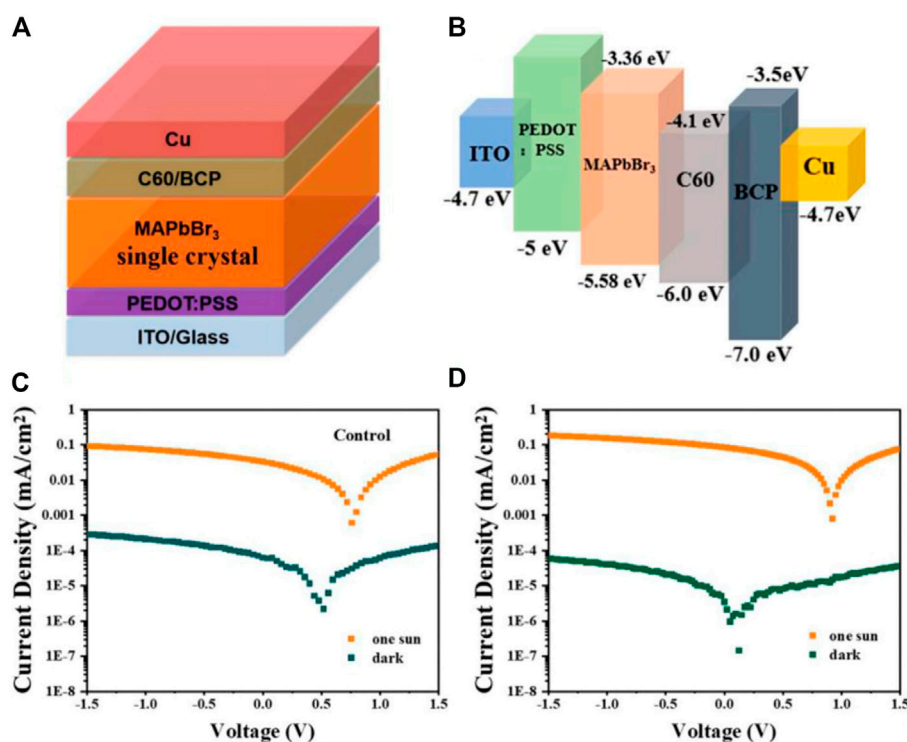


FIGURE 6

(A) Schematic diagram and (B) energy level of detector based on ITO/PEDOT: PSS/single crystals/C₆₀/BCP/copper (Cu). (C) With and without O₃-UV treated detector under dark and AM 1.5 illumination. Reproduced with permission from Ref. [44] (A) (B) (C) (D).

voltage can be applied because Schottky detectors work at reverse bias. Like a Schottky diode, when reverse bias is added, the depletion region extends and the leakage current level is low, thus promoting the charge collection and ensuring higher resolution [45].

3.1 Ohmic contacts

Ohmic contact promotes charge carrier transport. When Ohmic perovskite X-ray detectors work, an external bias was needed to drive ion migration. These symmetric devices have better performance at low bias voltage but present severe leakage (dark) current problems as the bias increases. For example, Au-perovskite-Au, a typical Ohmic contact structure, has been applied in recent researches. Chen *et al.* [46] have recorded electrical characteristics of the device with the structure of Au-(PEA)₄AgInBr₈ SCs-Au. They built a planar structure detector and made it exposed to X-ray with maximum energy of 50 keV, and a peak intensity of 30 keV. During the process (exposure dose rate: 34.5–138 μGy s⁻¹), no rectification was found from Figure 7A, showing a good Ohmic contact between Au electrode and (PEA)₄AgInBr₈. They tested the sensitivity of the device at 20, 100 and 200 V mm⁻¹, which was 21, 91 and 185 μC·Gy_{air}⁻¹ cm⁻¹ (Figure 7B). Under electric field of 20 V mm⁻¹, its dark current was 1.75 nA cm⁻² and dark current drift was 7.33 × 10⁻⁷ nA cm⁻¹.

Other examples like Au/Ag-Cs₂AgBiBr₆-Au/Ag also show some similar characteristics of ohmic detectors like relatively good sensitivity at low bias voltage and increase in dark current levels at high voltage. In

Pan *et al.* [47]'s research, Cs₂AgBiBr₆ detector with Au electrodes showed dark current of ~0.15 nA cm⁻² at 5 V and sensitivity ranging from 8 to 105 μC Gy_{air}⁻¹ cm⁻² (1 V–50 V bias). However, Dang *et al.* [48]'s work pointed out that the Ohmic contact behaviors between Au and Cs₂AgBiBr₆ are not perfect, resulting in obvious hysteretic *I-V* behaviors. Dang compared the energy level between Cs₂AgBiBr₆ single crystal and different metal electrodes including Au, Ag and Al, and constructed a better Ohmic contact of Ag with the Cs₂AgBiBr₆ SCs, which showed better photo-response and estimating detectivity (indicating the dark current level) of 1.38 × 10⁹ Jones in air.

Asymmetrical electrodes structures can also be applied in Ohmic detectors. According to Deumel *et al.* [49]'s work, the *J-E* plot (Figure 7C) showed typical Ohmic electrical behavior with the dark current density reaches the maximum value of 8.40 × 10⁻⁴ mA cm⁻² for negative fields and 1.98 × 10⁻³ mA cm⁻² for positive bias. This small difference may be attributed to asymmetrical electrodes and their different work functions ($\phi_{m,Cr} = 4.5$ eV and $\phi_{m,Pt} = 5.7$ eV). The maximum sensitivity of 9,300 μC·Gy_{air}⁻¹ cm⁻² has been witnessed under the electrical field of 0.17 V μm⁻¹, confirming the good sensitivity of Ohmic detectors with a low bias applied (Figure 7D).

3.2 Schottky contacts

In terms of perovskite X-ray detector, the high dark current level caused by 3D perovskites' ion migration is one of the main

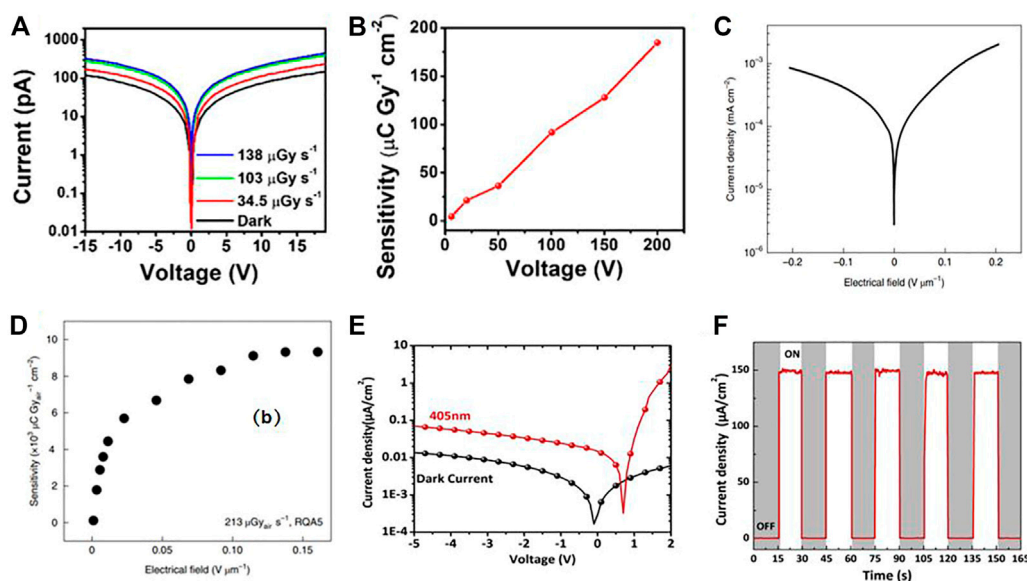


FIGURE 7

Photoelectric properties of perovskite X-ray detectors. (A) Dark (black) and response *current–voltage* (I – V) curves of the $(\text{PEA})_4\text{AgInBr}_8$ SCs detector at dose rates of 34.5, 103, and 138 $\mu\text{Gyair s}^{-1}$. (B) Dependence of X-ray sensitivity on applied voltage based on $(\text{PEA})_4\text{AgInBr}_8$ SCs detector. (C) Current density measurement under dark condition for an MAPbI_3 wafer. The applied voltage ranges from -200 to $+200$ V, which corresponds to an electrical field of ± 0.2 $\text{V } \mu\text{m}^{-1}$. (D) Calculated sensitivity (S) of the X-ray responses in the RQA5 spectrum and a dose of 213 $\mu\text{Gyair s}^{-1}$. Optical response: (E) Current–voltage (I – V) curve of the devices under dark atmosphere and a wavelength of 405 nm laser. (F) Photoresponse of the device under 405 nm laser with the power density of 0.636 mW/cm^2 at zero bias voltage. ON is the device under the exposure of laser. OFF is the device under a dark atmosphere. Reproduced with permission from Ref. [46] (A) (B), Ref. [50] (C) (D), Ref. [49] (E) (F).

obstacles that prevent it from practical application. One effective solution is to prevent it from practical application. One effective solution is to create asymmetrical electrode structures, forming Schottky barriers to suppress the severe ion migration problems. Recent researches about Schottky detectors have shown an enhancement in sensitivity and an decrease of dark current level at high bias voltage. Ag-perovskite-ITO sandwich structure is a commonly used strategy to create Schottky barriers for perovskite materials like MAPbBr_3 or CsPbBr_3 . In work of Xu *et al.* [50], the Schottky contact at the interface of $\text{MAPbBr}_3/\text{Ag}$ has been formed, whose typical electrical characteristics are revealed by the *current–voltage* (I – V) (Figure 7E), curve and the high and stable *On–Off* I – V behavior (Figure 7F), making it easier for electrons to cross the barrier and be collected by Ag. Moreover, with the barrier created by $\text{ITO}/\text{MAPbBr}_3$, a built-in electric field has been witnessed, promoting the photo-generated electron-hole pairs' separation, thus showing significant improvement in the response performance of the detector. They also test the detector's sensitivity with a bias voltage of 0 (35, 40, 45, 50 kV), which are 2.35×10^{-4} , 2.02×10^{-4} , 1.66×10^{-4} and 1.15×10^{-4} $\mu\text{C } \mu\text{Gyair}^{-1} \text{cm}^{-2}$ respectively. The dark current level can be demonstrated by the photoresponsivity (R), which is 22 mA/W in this case. Other Schottky X-ray detectors based on metal–perovskite–oxide semiconductor also exhibit high performances for X-ray detect. Xu *et al.* [51] replaced MAPbBr_3 with CsPbBr_3 to get a Schottky single crystal X-ray detector, which shows the Schottky behavior *current–voltage* (I – V) curve with the dark current density in the range of 5–25 nA/cm^2 (Figure 8A). Different from Ohmic detector, this

detector works at reverse voltage, with the sensitivity under inverse bias of -2 , -4 , -6 , and -8 V are 172, 292, 475, and 770 $\mu\text{C Gy}^{-1} \text{cm}^{-2}$, respectively (Figure 8C). Furthermore, under an X-ray dose rate of 333.69 $\mu\text{Gy}/\text{s}$, the sensitivity at different reverse biases is in the range of 0.07 – 2.86×10^3 $\mu\text{C}\cdot\text{Gyair}^{-1} \text{cm}^{-2}$ (Figure 8D). As shown in Figures 8A,B typical Schottky *On–Off* I – V behavior has been witnessed during the experiment.

Other researches focus on metal electrode structure. Xu *et al.* [52] used Al and Au to create Schottky contact and Ohmic contact. From the relationship of the exposure X-ray dose rate and the current response, the sensitivity at 50, 100, 150, and 200 V is up to 109, 204, 271, and 359 $\mu\text{C Gy}^{-1} \text{cm}^{-2}$. The response time is 76.2 ± 2.5 μs (200v, X-ray chopped at 2 kHz). The researchers later compare its electrical performance with an Ohmic detector with Au- MAPbBr_3 -Au (200 V bias, 50keV, 22.1 $\mu\text{Gy}/\text{s}$, whose sensitivity and response time are 62 $\mu\text{C Gy}^{-1} \text{cm}^{-2}$ and 272 ± 5 μs , confirming that Schottky detector's sensitivity and response time are higher or faster than Ohmic detector. The better electrical performances are mainly attributed to the Schottky barrier between Al and MAPbBr_3 SCs. This barrier could greatly suppress the leakage current at a high bias voltage, which allows higher electrical field (1.43×10^7 V/m) than Ohmic detector, thus achieving higher sensitivity.

For CsPbBr_3 , He *et al.* [53] applied Bi-perovskite-Au structure. Bi was made positive while Au being negative, forming large Schottky barriers on both metal–semiconductor interface under reversed bias, which greatly simultaneously blocked the charges' injection into the semiconductor and suppress the dark current level (on the order of 10^2 nA cm^{-2} at reverse bias voltage of 250 V cm^{-1}).

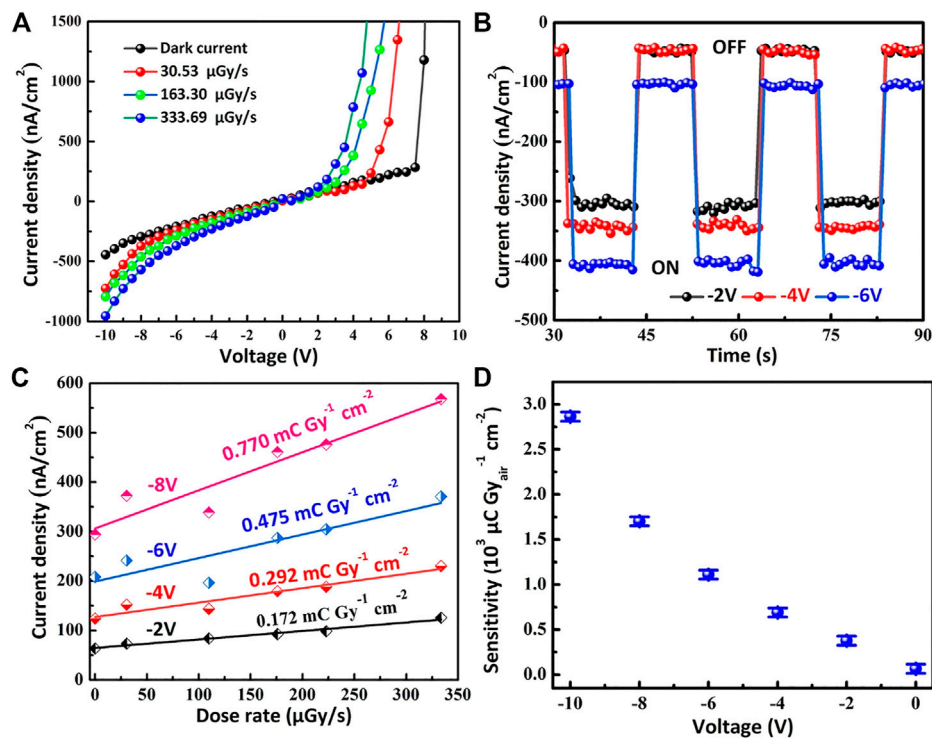


FIGURE 8

(A) I - V curve of CsPbBr₃ SCs devices under various X-ray dose rates (30.53, 163.30, and 333.69 $\mu\text{Gy/s}$). (B) On and off photocurrent density of CsPbBr₃ SCs devices with different biases applied (-2, -4, and -6 V) and irradiated by a 45 keV X-ray. (C) Photocurrent response of CsPbBr₃ SCs devices at different reverse biases under 40 keV X-ray various dose rates. (D) Sensitivity versus bias of CsPbBr₃ SCs devices under a 45 keV X-ray at the dose rate of 333.69 $\mu\text{Gy/s}$. Reproduced with permission from Ref. [51].

They then tested its sensitivity under various conditions (the X-ray tube voltage: 30–50 kV, the dose rate: 0.626 to $1.91 \times 10^4 \mu\text{C}\cdot\text{Gy}_{\text{air}}^{-1}$, which were in the range of few tens to over 8,000 $\mu\text{C}\cdot\text{Gy}_{\text{air}}^{-1} \text{cm}^{-2}$). The high Schottky barriers also enabled the device's self-powered X-ray detection with the sensitivity of $\sim 14 \mu\text{C}\cdot\text{Gy}_{\text{air}}^{-1} \text{cm}^{-2}$, which can be largely boosted to $\sim 192 \mu\text{C}\cdot\text{Gy}_{\text{air}}^{-1} \text{cm}^{-2}$ if 1 V reverse bias is applied.

4 Summary and perspective

Generally speaking, great strides have been achieved in perovskite-based X-ray detector. In this work, we have surveyed recent development of perovskite materials and devices for performance improvement of X-ray detector. There exists some representative examples where high sensitivity have been realized, and low limit detection have been reached. Concerning the materials modification, researchers mainly focus on interstitially doping, epitaxial wide band gap semiconductors, organic carriers transport layer to suppress dark current. We're hopeful for upcoming researches that exploit more metal cationic dopants, polymers and other small organic molecules to modify the material. And the wide band gap semiconductor can be activated by narrow-band gap semiconductor to optimize the driving force of electron transport through quantum confinement effect. Hence, it is

suggested to improve the detection performance. Furthermore, to design band structure of heterojunction, Type-II is expected for favorable charge separation, driving the perovskite-based X-ray detector to higher level. Whether organic material or inorganic salts are welcomed to be paired with perovskite, even 2D materials are desired to be employed. As for the device structure, the p-i-n device attributed to its high sensitivity, is superior to MSM one. Fortunately, the performance of MSM device can be improved through adopting double layer perovskite. Notably, based on the similarity, the materials and devices applied in photovoltaic field are valuable for reference.

Ohmic and Schottky contacts were also mainly investigated for electrode-perovskite contacts in recent studies. In these researches, Ohmic contact enables great stability but high dark current while Schottky contact demands higher voltage bias but shows the ability of dark current suppression. Metal materials, device structure and energy level should be considered for desired properties of carrier transportation. At same time, more efforts should be paid to dig in-depth mechanisms of electrodes interface to understand more clearly.

In summary, further researches are expected to enhance the sensitivity and response speed while decreasing the limit of detection. And proper material band and device structure design will lay foundation for commercial and large-scale perovskite X-ray detector.

Author contributions

YH summarized the papers and wrote the introduction and band theory. ZW wrote band engineering with heterojunction and summary. ZW wrote perovskite X-ray detectors with Electrode contact. All authors discussed the results and commented on the manuscript.

Funding

This work was supported by Beijing Natural Science Foundation (M22020), the National Key R&D Program (2020YFA0709800) and National Natural Science Foundation (U20A20168, 51861145202, 61874065, 62022047) of China. HT is grateful for the support of Fok YingTong Education Foundation (Grant No. 171051), Beijing National Research Center for Information Science and Technology Youth Innovation Fund (BNR2021RC01007), State Key Laboratory of New Ceramic and Fine Processing Tsinghua

References

- Kasap SO, Rowlands JA. Direct-conversion flat-panel X-ray image sensors for digital radiography. *Proc IEEE* (2002) 90(4):591–604. doi:10.1109/jproc.2002.1002529
- Wei HT, Huang JS. Halide lead perovskites for ionizing radiation detection. *Nat Commun* (2019) 10:1066. doi:10.1038/s41467-019-08981-w
- Chen QS, Wu J, Ou X, Huang B, Almutlaq J, Zhumekenov AA, et al. All-inorganic perovskite nanocrystal scintillators. *Nature* (2018) 561(7721):88–93. doi:10.1038/s41586-018-0451-1
- Zhou Y, Chen J, Bakr OM, Mohammed OF. Metal halide perovskites for X-ray imaging scintillators and detectors. *ACS Energy Lett* (2021) 6(2):739–68. doi:10.1021/acenergylett.0c02430
- Xia M, Yuan J, Niu G, Du X, Yin L, Pan W, et al. Unveiling the structural descriptor of AX₉ perovskite derivatives toward X-ray detectors with low detection limit and high stability. *Adv Funct Mater* (2020) 30(24):1910648. doi:10.1002/adfm.201910648
- Wangyang PH, Gong C, Rao G, Hu K, Wang X, Yan C, et al. Recent advances in halide perovskite photodetectors based on different dimensional materials. *Adv Opt Mater* (2018) 6(11):1701302. doi:10.1002/adom.201701302
- Sun SB, Yuan D, Xu Y, Wang A, Deng Z. Ligand-mediated synthesis of shape-controlled cesium lead halide perovskite nanocrystals via reprecipitation process at room temperature. *ACS Nano* (2016) 10(3):3648–57. doi:10.1021/acsnano.5b08193
- Zhao W, Rowlands JA. X-ray imaging using amorphous selenium: Feasibility of a flat panel self-scanned detector for digital radiology. *Med Phys* (1995) 22(10):1595–604. doi:10.1118/1.597628
- Kasap SO. X-Ray sensitivity of photoconductors: Application to stabilized a-Se. *J Phys D-Applied Phys* (2000) 33(21):2853–65. doi:10.1088/0022-3727/33/21/326
- Keshavarz M, Debroye E, Ottesen M, Martin C, Zhang H, Fron E, et al. Tuning the structural and optoelectronic properties of Cs₂AgBiBr₆ double-perovskite single crystals through alkali-metal substitution. *Adv Mater* (2020) 32(40):2001878. doi:10.1002/adma.202001878
- Yan J, Gao F, Tian Y, Li Y, Gong W, Wang S, et al. Controllable perovskite single crystal heterojunction for stable self-powered photo-imaging and X-ray detection. *Adv Opt Mater* (2022) 10(17):2200449. doi:10.1002/adom.202200449
- Yakunin S, Dirin DN, Shynkarenko Y, Morad V, Cherniukh I, Nazarenko O, et al. Detection of gamma photons using solution-grown single crystals of hybrid lead halide perovskites. *Nat Photon* (2016) 10(9):585–9. doi:10.1038/nphoton.2016.139
- Yang B, Pan W, Wu H, Niu G, Yuan JH, Xue KH, et al. Heteroepitaxial passivation of Cs₂AgBiBr₆ wafers with suppressed ionic migration for X-ray imaging. *Nat Commun* (2019) 10(1):1989–10. doi:10.1038/s41467-019-09968-3
- Yan KR, Chen J, Ju H, Ding F, Chen H, Li CZ. Achieving high-performance thick-film perovskite solar cells with electron transporting Bingel fullerenes. *J Mater Chem A* (2018) 6(32):15495–503. doi:10.1039/c8ta05636f
- He X, Xia M, Wu H, Du X, Song Z, Zhao S, et al. Quasi-2D perovskite thick film for X-ray detection with low detection limit. *Adv Funct Mater* (2022) 32(7):2109458. doi:10.1002/adfm.202109458
- Zhuang RZ, Wang X, Ma W, Wu Y, Chen X, Tang L, et al. Highly sensitive X-ray detector made of layered perovskite-like (NH₄)₃Bi₂I₉ single crystal with anisotropic response. *Nat Photon* (2019) 13(9):602–8. doi:10.1038/s41566-019-0466-7
- Zhang JY, Li A, Li B, Yang M, Hao X, Wu L, et al. Top-seed solution-based growth of perovskite Cs₃Bi₂I₉ single crystal for high performance X-ray detection. *ACS Photon* (2022) 9(2):641–51. doi:10.1021/acsp Photonics.1c01647
- Yin WJ, Shi TT, Yan YF. Unusual defect physics in CH₃NH₃PbI₃ perovskite solar cell absorber. *Appl Phys Lett* (2014) 104(6):063903. doi:10.1063/1.4864778
- He YH, Pan W, Guo C, Zhang H, Wei H, Yang B. 3D/2D perovskite single crystals heterojunction for suppressed ions migration in hard X-ray detection. *Adv Funct Mater* (2021) 31(49):2104880. doi:10.1002/adfm.202104880
- Karl N. Charge carrier transport in organic semiconductors. *Synth Met* (2003) 133: 649–57. doi:10.1016/s0379-6779(02)00398-3
- Hu ZS, Lin Z, Su J, Zhang J, Chang J, Hao Y. A review on energy band-gap engineering for perovskite photovoltaics. *Solar Rrl* (2019) 3(12):1970116. doi:10.1002/solr.201970116
- Xie JS, Hang P, Wang H, Zhao S, Li G, Fang Y, et al. Perovskite bifunctional device with improved electroluminescent and photovoltaic performance through interfacial energy-band engineering. *Adv Mater* (2019) 31(33):1902543. doi:10.1002/adma.201902543
- Pan Y, Wang X, Zhao J, Xu Y, Li Y, Li Q, et al. Photodiodes based on a MAPbBr₃/Bi³⁺-doped MAPbCl₃ single crystals heterojunction for the X-ray detection. *CrystEngComm* (2021) 23(28):4954–62. doi:10.1039/d1ce00406a
- Ulatowski AM, Wright AD, Wenger B, Buizza LRV, Motti SG, Eggimann HJ, et al. Charge-carrier trapping dynamics in bismuth-doped thin films of MAPbBr₃ perovskite. *J Phys Chem Lett* (2020) 11(9):3681–8. doi:10.1021/acs.jpclett.0c01048
- Yamada Y, Hoyano M, Akashi R, Oto K, Kanemitsu Y. Impact of chemical doping on optical responses in bismuth-doped CH₃NH₃PbBr₃ single crystals: Carrier lifetime and photon recycling. *J Phys Chem Lett* (2017) 8(23):5798–803. doi:10.1021/acs.jpclett.7b02508
- Kamat PV. Semiconductor nanocrystals: To dope or not to dope. *J Phys Chem Lett* (2011) 2(21):2832–3. doi:10.1021/jz201345y
- Zheng Z, Zu X, Zhang Y, Zhou W. Rational design of type-II nano-heterojunctions for nanoscale optoelectronics. *Mater Today Phys* (2020) 15:100262. doi:10.1016/j.mphys.2020.100262
- Wei W, Zhang Y, Xu Q, Wei H, Fang Y, Wang Q, et al. Monolithic integration of hybrid perovskite single crystals with heterogenous substrate for highly sensitive X-ray imaging. *Nat Photon* (2017) 11(5):315–21. doi:10.1038/nphoton.2017.43
- Li LQ, Fang YJ, Yang DR. Interlayer-assisted growth of Si-based all-inorganic perovskite films via chemical vapor deposition for sensitive and stable X-ray detection. *J Phys Chem Lett* (2022) 13(24):5441–50. doi:10.1021/acs.jpclett.2c01389
- Zhang XY, Zhu T, Ji C, Yao Y, Luo J. *In situ* epitaxial growth of centimeter-sized lead-free (BA)₂CsAgBiBr₇/Cs₂AgBiBr₆ heterocrystals for self-driven X-ray detection. *J Am Chem Soc* (2021) 143(49):20802–10. doi:10.1021/jacs.1c08959

University (No. KF202109), and Tsinghua-Foshan Innovation Special Fund (TFISF) (2021THFS0217).

Conflict of interest

The authors declare that the research was conducted in the absence of any commercial or financial relationships that could be construed as a potential conflict of interest.

Publisher's note

All claims expressed in this article are solely those of the authors and do not necessarily represent those of their affiliated organizations, or those of the publisher, the editors and the reviewers. Any product that may be evaluated in this article, or claim that may be made by its manufacturer, is not guaranteed or endorsed by the publisher.

31. Xu YK, Li Y, Peng G, Wang Q, Li Z, Wang H, et al. Asymmetric metal halide film with suppressed leakage current for high sensitive X-ray detection and imaging. *Ieee Electron Device Lett* (2022) 43(10):1709–12. doi:10.1109/led.2022.3202173
32. Kim J, Johnson W, Kanakaraju S, Lee CH. Lateral InP/InGaAs double heterojunction phototransistor over a trench interdigitated finger structure. *Solid-State Electron* (2007) 51(7):1023–8. doi:10.1016/j.sse.2007.05.010
33. Brennan KF, Haralson J, Parks JW, Salem A. Review of reliability issues of metal-semiconductor-metal and avalanche photodiode photonic detectors. *Microelectronics Reliability* (1999) 39(12):1873–83. doi:10.1016/s0026-2714(99)00197-3
34. Wei JJ, Tao L, Li L, Yan M, Wang C, Sun W, et al. Tuning the photon sensitization mechanism in metal-halide-perovskite-based nanocomposite films toward highly efficient and stable X-ray detection. *Adv Opt Mater* (2022) 10(7):2102320. doi:10.1002/adom.202102320
35. Wang JH, Fu S, Huang L, Lu Y, Liu X, Zhang J, et al. Heterojunction engineering and ideal factor optimization toward efficient MINP perovskite solar cells. *Adv Energy Mater* (2021) 11(48):2102724. doi:10.1002/aenm.202102724
36. Song YL, Li L, Hao M, Bi W, Wang A, Kang Y, et al. Elimination of interfacial-electrochemical-reaction-induced polarization in perovskite single crystals for ultrasensitive and stable X-ray detector arrays. *Adv Mater* (2021) 33(52):2103078. doi:10.1002/adma.202103078
37. Xu XW, Qian W, Wang J, Yang J, Chen J, Xiao S, et al. Sequential growth of 2D/3D double-layer perovskite films with superior X-ray detection performance. *Adv Sci* (2021) 8(21):2102730. doi:10.1002/advs.202102730
38. Zhou Y, Zhao L, Ni Z, Xu S, Zhao J, Xiao X, et al. Heterojunction structures for reduced noise in large-area and sensitive perovskite x-ray detectors. *Sci Adv* (2021) 7(36):eabg6716. doi:10.1126/sciadv.abg6716
39. Cui F, Zhang P, Zhang L, Hua Y, Sun X, Li X, et al. Liquid-phase epitaxial growth of large-area MAPbBr_{3-n}Cl_n/CsPbBr₃ perovskite single-crystal heterojunction for enhancing sensitivity and stability of X-ray detector. *Chem Mater* (2022) 34(21):9601–12. doi:10.1021/acs.chemmater.2c02266
40. Dun GH. Cs₂AgBiBr₆ -Tellurium heterojunction-based high-performance X-ray detectors. In: 6th IEEE Electron Devices Technology and Manufacturing Conference (EDTM). Electr Network (2022).
41. Kaushik S, Naik TR, Alka A, Garg M, Tak BR, Ravikanth M, et al. Surface modification of AlN using organic molecular layer for improved deep UV photodetector performance. *Acs Appl Electron Mater* (2020) 2(3):739–46. doi:10.1021/acsaelm.9b00811
42. Franciosi A, Van de Walle CG. Heterojunction band offset engineering. *Surf Sci Rep* (1996) 25(1–4):1–140. doi:10.1016/0167-5729(95)00008-9
43. Gao ZW, Wang Y, Choy WCH. Buried interface modification in perovskite solar cells: A materials perspective. *Adv Energy Mater* (2022) 12(20):2104030. doi:10.1002/aenm.202104030
44. Feng A, Xie S, Fu X, Chen Z, Zhu W. Inch-sized thin metal halide perovskite single-crystal wafers for sensitive X-ray detection. *Front Chem* (2022) 9:823868. doi:10.3389/fchem.2021.823868
45. Gnatyuk V, Maslyanchuk O, Solovan M, Brus V, Aoki T. CdTe X/y-ray detectors with different contact materials. *Sensors* (2021) 21(10):3518. doi:10.3390/s21103518
46. Chen D, Niu G, Hao S, Fan L, Zhao J, Wolverson C, et al. Decreasing structural dimensionality of double perovskites for phase stabilization toward efficient X-ray detection. *ACS Appl Mater Inter* (2021) 13(51):61447–53. doi:10.1021/acsaami.1c20234
47. Pan WC, Wu H, Luo J, Deng Z, Ge C, Chen C, et al. Cs₂AgBiBr₆ single-crystal X-ray detectors with a low detection limit. *Nat Photon* (2017) 11(11):726–32. doi:10.1038/s41566-017-0012-4
48. Dang YY, Tong G, Song W, Liu Z, Qiu L, Ono LK, et al. Interface engineering strategies towards Cs₂AgBiBr₆ single-crystalline photodetectors with good Ohmic contact behaviours. *J Mater Chem C* (2020) 8(1):276–84. doi:10.1039/c9tc04780h
49. Deumel S, van Breemen A, Gelinck G, Peeters B, Maas J, Verbeek R, et al. High-sensitivity high-resolution X-ray imaging with soft-sintered metal halide perovskites. *Nat Electron* (2021) 4(9):681–8. doi:10.1038/s41928-021-00644-3
50. Xu Q, Zhang B, Nie J, Zhang H, Ouyang X, Liu J, et al. Self-powered X-ray detector based on methylammonium lead tribromide single crystals. *J Alloys Comp* (2021) 859:157826. doi:10.1016/j.jallcom.2020.157826
51. Xu Q, Wang X, Zhang H, Shao W, Nie J, Guo Y, et al. CsPbBr₃ single crystal X-ray detector with Schottky barrier for X-ray imaging application. *Acs Appl Electron Mater* (2020) 2(4):879–84. doi:10.1021/acsaelm.9b00832
52. Xu Q, Shao W, Li Y, Zhang X, Ouyang X, Liu J, et al. High-performance surface barrier X-ray detector based on methylammonium lead tribromide single crystals. *Acs Appl Mater Inter* (2019) 11(10):9679–84. doi:10.1021/acsaami.8b21605
53. He YH, Hadar I, De Siena MC, Klepov VV, Pan L, Chung DY, et al. Sensitivity and detection limit of spectroscopic-grade perovskite CsPbBr₃ crystal for hard X-ray detection. *Adv Funct Mater* (2022) 32(24):2112925. doi:10.1002/adfm.202112925